Available online at www.sciencedirect.com

SCIENCE DIRECT®

Journal of Volcanology and Geothermal Research 138 (2004) 127–138

Journal of volcanology and geothermal research

www.elsevier.com/locate/jvolgeores

Rhyodacitic fissure eruption in Southern Andes (*Cordón Caulle*; 40.5°S) after the 1960 (Mw:9.5) Chilean earthquake: a structural interpretation

L.E. Lara[a,b,*], J.A. Naranjo[a], H. Moreno[a]

[a]*SERNAGEOMIN, Servicio Nacional de Geología y Minería, Chile*
[b]*Université Paul Sabatier, Toulouse III, France*

Received 16 October 2003; accepted 22 June 2004

Abstract

The 1960 rhyodacitic fissure eruption in the *Cordón Caulle* Volcanic Complex (CCVC), located in Southern Andes (40.5°S) was a unique volcanic episode. The remarkable eruption was triggered by the greatest recorded subduction-zone earthquake, starting 38 h after the main shock, 240 km inland. The structural behaviour, two compound fissures opening along a margin-oblique (NW) structure related to the Quaternary evolution of the CCVC, suggests that the prefractured nature of the upper crust in the Southern Andes was an influential condition for volcanic eruptions. From historical data and morphologic and structural analysis, we suggest that NW structures constitute pathways of steady magmatic ascent. Thus, during the great seismic event, and catalysed by the fluid pressure around a fault, it would have been reactivated allowing, initially, the propagation of a non-Andersonian dyke. Then, the silicic magma would have reached the surface by 'seismic pumping'. Once the initial activity in the reactivated segments ceased, the local stress field would have changed, favouring the formation of new failures, this time almost parallel to the maximum horizontal stress, and promoting magma transport as Andersonian dykes. Although the rheologic characteristics of the silicic lavas erupted together with the structural behaviour and seismic features of this eruptive cycle constitute rather exceptional conditions in the Southern Andes record, the prefractured nature of the upper crust and the shifting propagation of Andersonian and non-Andersonian dykes provide a theoretical framework to analyse the neotectonics of the volcanic arc in a convergent margin.

Keywords: fissure eruption; rhyodacitic magma; 1960 Chilean earthquake; fault reactivation

1. Introduction

The relationship between volcanism and tectonics has been a controversial topic for many years. The early recognition of close spatial relationships

* Corresponding author. Av. Santa Maria 0104, Providencia-Santiago, Chile.
E-mail address: lelara@sernageomin.cl (L.E. Lara).

0377-0273/$ - see front matter © 2004 Elsevier B.V. All rights reserved.
doi:10.1016/j.jvolgeores.2004.06.009

between faults and volcanic centres has led to construction of models that try to explain the pattern of regional deformation as well as the distribution, evolution and morphostructure of the volcanic centres in different geodynamic settings (Takada, 1994; Bellier and Sébrier, 1994; Dhont et al., 1998). For example, Nakamura (1977) suggested that the parasitic cones of stratovolcanoes are aligned according to the maximum horizontal stress (σ_{hmax}). Other authors have shown direct links between the geometry of the faults that are used as pathways for magmatic ascent (Tibaldi, 1995), their displacements (e.g., Delaney et al., 1986; Alaniz-Alvarez et al., 1998), and some morphologic characteristics of the volcanic centres. Although that is a key topic of research in the Southern Andes Volcanic Zone (SAVZ: 33–46°S), we want to focus on two less discussed aspects: (1) the reactivation of structures allowing the emplacement of 'non-Andersonian' dykes (i.e. dykes not parallel to σ_{hmax} and therefore not correspond to 'Andersonian' structures; Anderson, 1951; Bahar and Girod, 1983; Delaney et al., 1986) and (2) injection resulting from coseismic deformation during large earthquakes in subduction zones. The concept of fault reactivation was mainly developed by Sibson (1985, 1987, 1996, 2000) and Sibson et al. (1988) to explain cycles of mineralization in several tectonic settings and is an important framework for understanding prefractured convergent margins with regional-scale active faults. This is the case of the South Southern Volcanic Zone (SSAVZ: 37–46°S) where the Quaternary volcanic arc has been built close to trench-parallel Cenozoic structures such as the Liquiñe-Ofqui Fault (e.g., Cembrano et al., 1996; Lavenu and Cembrano, 1999), as well as, older NW–SE structures, possibly formed previous to the Mesozoic Andean cycle.

In addition, coseismic deformation propagated inland for 250 km would be an unlikely fact, although it is possible in the context of the largest earthquake instrumentally recorded in the world (rupture zone around 1000 km long) (Fig. 1). The relation between subduction earthquakes and volcanic eruptions has been analysed by Blot (1965), Acharya (1982) and Linde and Sacks (1998), among others, although with very different data sets. Although the instantaneous deformation in the volcanic arc in the Southern Andes was not monitored during the 1960 eruptive cycle,

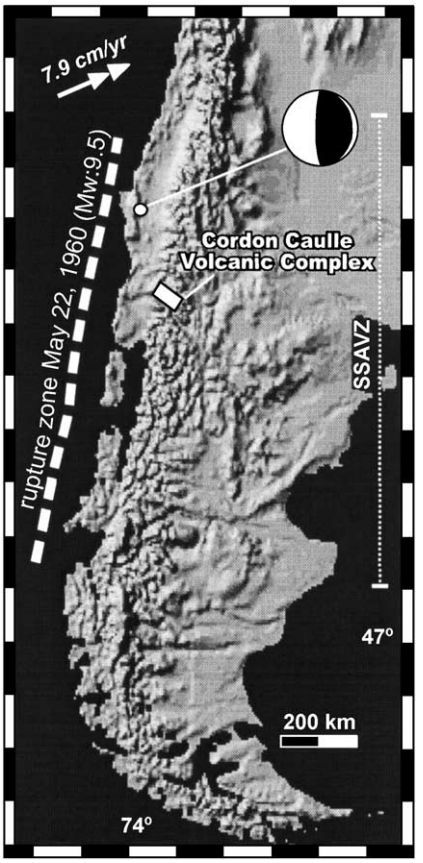

Fig. 1. Shaded relief of South America. White box shows the CCVC. Rupture zone of 1960 Chilean earthquake after Plafker and Savage (1970) and relocated epicentre (Cifuentes, 1989) are shown. Current subduction velocity after DeMets et al. (1994) is also indicated. A focal mechanism solution for 1960 earthquake by Cifuentes (1989) is at upper right corner (black region corresponds to compression on lower hemisphere diagram).

some morphologic features, as well as the analysis of several technical reports and papers (Veyl, 1960; Saint Amand, 1961; Casertano, 1962; Katsui and Katz, 1967) about the eruptive process, allow a more comprehensive explanation of the eruptive event as a whole. A structural analysis based on the classic theory of fractures and brittle rupture criteria (e.g., Anderson, 1951; Hubbert and Rubey, 1959; Byerlee, 1978) together with new approaches on fault reshearing (e.g., Sibson, 1985, 1987, 1996, 2000; Sibson et al., 1988) may explain the relationship between the coseismic deformation and the fissure eruption of a rhyodacitic magma.

2. Cordón Caulle Volcanic Complex (CCVC)

Cordón Caulle Volcanic Complex (CCVC) is a cluster of eruptive centres that extends between the Cordillera Nevada caldera (1799 m a.s.l.) and the Puyehue stratovolcano (2236 m a.s.l.) from NW to SE (Fig. 2). It consists of various fissure vents with aligned domes and pyroclastic cones (Moreno, 1977). The CCVC, located 240 km east of the Chile–Perú trench, forms a transversal 15 km long by 4 km wide ridge of 135° azimuthal direction, including a nested graben. On the northwestern end is located the Cordillera Nevada caldera, a collapsed Pleistocene stratovolcano (Campos et al., 1998; Lara et al., 2001, 2003) while on the southeastern end, the Puyehue stratovolcano appears as a prominent truncated cone that has a 2.5-km diameter summit caldera intermittently active during the last 10,000 years with noticeable explosive pulses. The chemical composition of the CCVC has been mainly rhyodacitic to rhyolitic (68–71% SiO_2; Gerlach et al., 1988), with subordinated basaltic to andesitic types among the earlier lavas. The abundance of silicic types is unique among the mostly bimodal centres along the SSAVZ

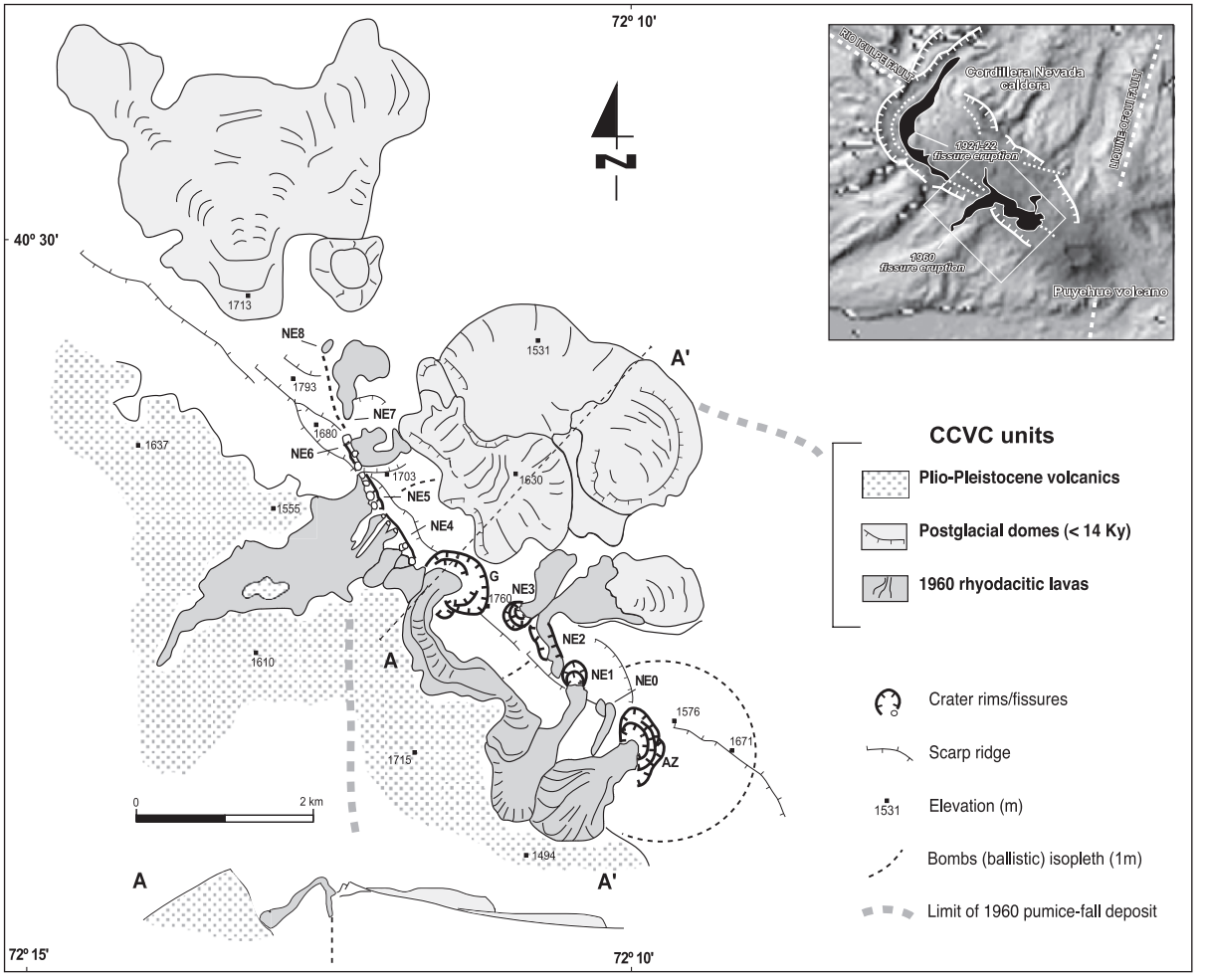

Fig. 2. Geologic map of 1960 fissure in the CCVC. Main crater, fissure or vents are labelled (G: Gris crater; AZ: El Azufral crater; NE0, NE1, NE3, NE7 and NE8 vents; NE2, NE4; NE5 and NE6 fissures). Insert sketch shows CCVC as a whole (white box is the map area) and 1921–22 and 1960 fissure vents. Regional long-lived faults are also indicated.

(37–46°S), where basalts widely predominate over more silica-rich rocks.

The tectonic control of the CCVC seems to be remarkable. The entire volcanic complex was built on a pre-Andean NW structure that limits geological domains at regional scale. For example, the overall construction of Puyehue volcano was coeval with the early stages of lava domes eruptions along the internal NW graben in the CCVC (Moreno, 1977). Moreover, another fissure eruption of rhyodacitic magma in 1922 is recognized in the northwestern end of the CCVC where NW fissures bend as ring faults inside the Cordillera Nevada caldera. On the other hand, several hot springs, forming the most important active geothermal field of the SSAVZ, are located inside the graben that joins Cordillera Nevada caldera with the Puyehue stratovolcano (Fig. 2). In the CCVC, microseismic volcanotectonic events, together with long period and low frequency signals and a sustained tremor may be related to the opening and closing of the hydrothermal and magma conduits inside the structural system (Peña and Fuentealba, 2000).

3. The 1960 earthquake (Mw=9.5)

The 1960 Chilean earthquake is the largest instrumentally recorded in the world. The magnitude of the released energy saturated the conventional scale when the dimension of the rupture zone exceeded the wavelength of the seismic waves used for its calculation (Kanamori and Cipar, 1974). Thus, Kanamori (1977) proposed a new scale that considers the seismic moment for the equation of energy of Gutenberg–Richter (Gutenberg, 1956). In this modified scale, the Chilean earthquake of 1960 reaches Mw=9.5, followed by the Alaska 1964 (Mw=9.2), Aleutians 1957 (Mw=9.1) and Kamchatka 1952 (Mw=9.0) earthquakes. The rupture zone (Fig. 1), determined by Plafker and Savage (1970) considering coseismic intensities and land deformations, reaches 1000 km in length, with the CCVC located approximately in front of the middle of this segment. Some of the effects of the earthquake were worldwide and, for example, Smylie and Mansinha (1968) described a shift of the terrestrial axis of rotation that followed the earthquake and Eaton et al. (1961), Sievers et al. (1963), and Berninghausen (1962) described destructive tsunamis that affected the coasts of the western Pacific Ocean. In addition, Duda (1963) and Plafker and Savage (1970) made a detailed compilation of the sequence of seismic events that began on May 21st (10:03 GMT), with a first shock located in the north end of the rupture zone, and culminated on May 22nd (19:11 GMT) with the main shock, whose epicentre was located 140 km toward the southwest of the first one. More recently, Cifuentes (1989) analysed the foreshock and aftershock sequences constraining the source mechanism of the main thrust event. Many authors (e.g., Veyl, 1960; Weischet, 1963) report huge topographic changes along the Pacific shoreline where up to 5.7 m of uplift and 2.7 m of subsidence occurred after the main earthquake. Subsequently, using a local geodetic network, Plafker and Savage (1970) characterized the coseismic deformation in the coastal area and inland. In addition to uplift and subsidence along the shoreline, spontaneous water springs, 'mud volcanoes' and cracks, took place on the unconsolidated deposits. Fractures up to 500 m long with orthogonal directions of N45° and N135° were recognized in the coastal area. Landslides located along the main trace of the Liquiñe–Ofqui Fault were the easternmost morphologic effects of the 1960 earthquake.

Only 38 h after the main shock, an eruptive cycle of the CCVC began. Although the Chilean seismic network available in 1960 was too sparse to suitably characterize the earthquake sequence, the zone of continental surficial deformation was at least 150 km wide according to the local geodetic network (Plafker and Savage, 1970). With these data, Barrientos and Ward (1990) obtained the displacement in the rupture zone. Using this displacement, Barrientos (1994) made a bidimensional analysis of the deformation and applied a static propagator matrix (Ward, 1984) to obtain the displacements in the CCVC area, assuming a 25° west vergent thrust plane in the rupture zone. If their assumptions were correct, horizontal displacements of ca. 20 m in the coastal area, close to the rupture zone, suitably fit the measured vertical variations and could have produced EW horizontal displacement of ca. 2 m in the main cordillera, where the CCVC is located. Following this analysis, displacements sufficiently large to reactivate shallow

structures and to trigger the CCVC eruption seem plausible.

4. 1960 fissure CCVC eruption

The isolated area where CCVC is located made the direct observation of the 1960 eruptive cycle difficult. In addition, because of the fatalities and the huge damage caused by the earthquake itself, there were few recorded reports of the eruption. Nevertheless, the reviews of newspaper articles, technical reports (Veyl, 1960; Saint Amand, 1961; Casertano, 1962; Katsui and Katz, 1967), an unpublished thesis (Moreno, 1977) and new precise geomorphologic field observations, have allowed its characterization.

The 1960 eruptive cycle (Table 1) occurred on a ca. 5.5-km long N135° fissure located near the SW margin of the CCVC and was formed by two sub-parallel segments. Each of these segments has secondary alignments oriented N160–165°. Twenty-one identifiable vents emitted pyroclastic ejecta and lava flows of rhyodacitic composition (68.9–70.01% SiO_2) with a ca. 0.25 km^3 of DRE volume. The eruptive cycle began on May 24th (09:00 h GMT), 38 h after the main shock of May 22nd, starting with an explosive subplinian phase and the formation of an eruptive 'mushroom-like' column about 8 km high, together with the emission of water vapour from other vents along the fissure system. The most active centre in this phase (stage 1) was the Gris crater (Figs. 2 and 3), followed by El Azufral crater (Fig. 2), both at the tips of the fissure. The pyroclastic plumes were dispersed toward the southeast forming a white pumice deposit with thickness up to 10 cm at 30–40 km of the Gris crater. An accumulation of 'bread crust' bombs and coarse lapilli pumice around the Gris crater formed a low aspect ratio pyroclastic cone.

Table 1
Summary of 1960 eruptive cycle

	May 21st (10:03 GMT)	Foreshock in the north end of rupture zone of 1960 earthquake
	May 22nd (19:11 GMT)	Main shock of 1960 earthquake
Stage 1	May 24th (09:00 GMT)	Subplinian phase on N135 alignments: pyroclastic ejecta from Gris and Azufral craters
Stage 2	May 26th?	Effusive phase on N135 alignments: rhyodacitic lava from Gris, NE1 and Azufral craters
Stage 3	June?	Effusive phase on N165 alignments: rhyodacitic lava from NE2 to NE8 vents; rhyodacitic lava from Gris, NE1 and Azufral craters continued
	June	Effusive ongoing phase
	July?	Quiescence period
	pre-July 22nd	Renewed pyroclastic phase: ballistic ejecta from Gris and Azufral craters
	post-July 22nd–present	Quiescence period/Solfataric and microseismic activity

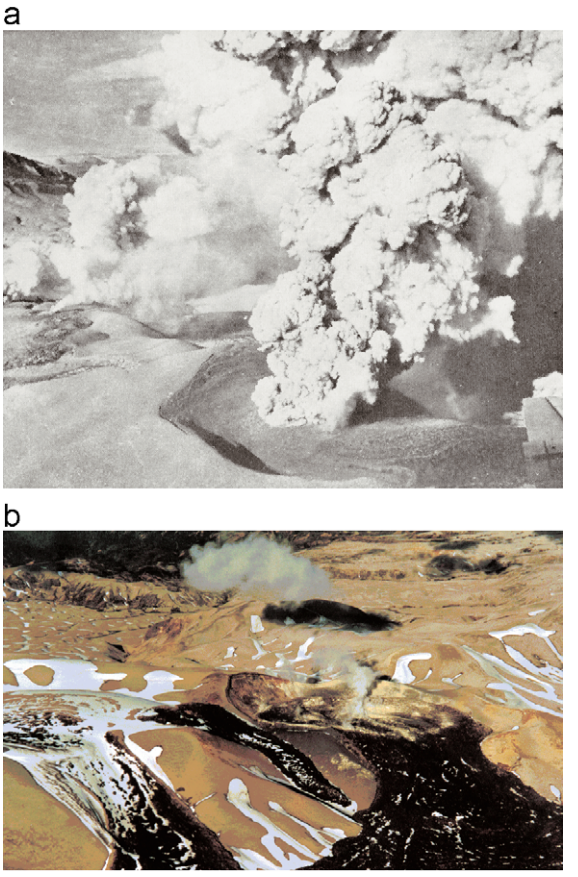

Fig. 3. (a) Aerial photograph of the 1960 eruptive cycle in the CCVC (P. Saint Amand in Casertano, 1962). This picture, taken toward the southwest, shows the Gris crater in close-up view and the coeval water vapour columns through northeastern vents (NE2; NE3) during the third eruptive stage. (b) Current aerial view of El Azufral crater, NE0 and NE1 vents with a still active solfatara, 44 years later.

An effusive phase, with emission of *a′a* and blocky rhyodacitic clinopyroxene and Fe-olivine lava flows followed the previous stage. The first blocky lava flow was produced by NE1 crater (Fig. 2), followed by the coeval flows from the Gris and El Azufral craters. The eruptive vents evolved to a N160–165° (stage 3) alignments (NE2 and NE4 vents), as the first phase culminated. A compound *a′a* lava flow, fed from NE5 craters, was emplaced toward the SW of the fissure. As these vents were sealed by viscous lava flows, a quiescence period followed and renewed activity started with an explosive phase characterized by the accumulation of 'bread crust' bombs (0.5–1.0 m diameter) around the Gris and El Azufral craters, apparently the only active ones during this latest phase. Ballistic ejecta cover a coarse lapilli pumice-fall deposit that represents the proximal facies of an eruptive column during the last phase, which ended on July 22nd after 2 months of activity.

5. Morphometric analysis

To better understand the structural conditions during each eruptive cycle, we measured such morphometric parameters as vent alignments, elongation axes of pyroclastic cones and craters, cone breaching or collapse directions (Fig. 4) and then, we interpreted them within the context of existing analogue models (e.g.,Tibaldi, 1995).

The alignment of the major craters along the N135° direction arises as a first order feature. All vents lie on a ridge which flanks slope 40–50° southwest and 10–20° northeast, the axis of which parallels the alignments of larger emission centres and postglacial rhyolitic domes. The elongation of Gris pumice cone is parallel to the main direction (135°) and the crater elongation of major vents (Gris and El Azufral), as well as their internal depressions, is parallel to both the main N135° and the secondary N160–165° directions. All the emission centres without open craters are

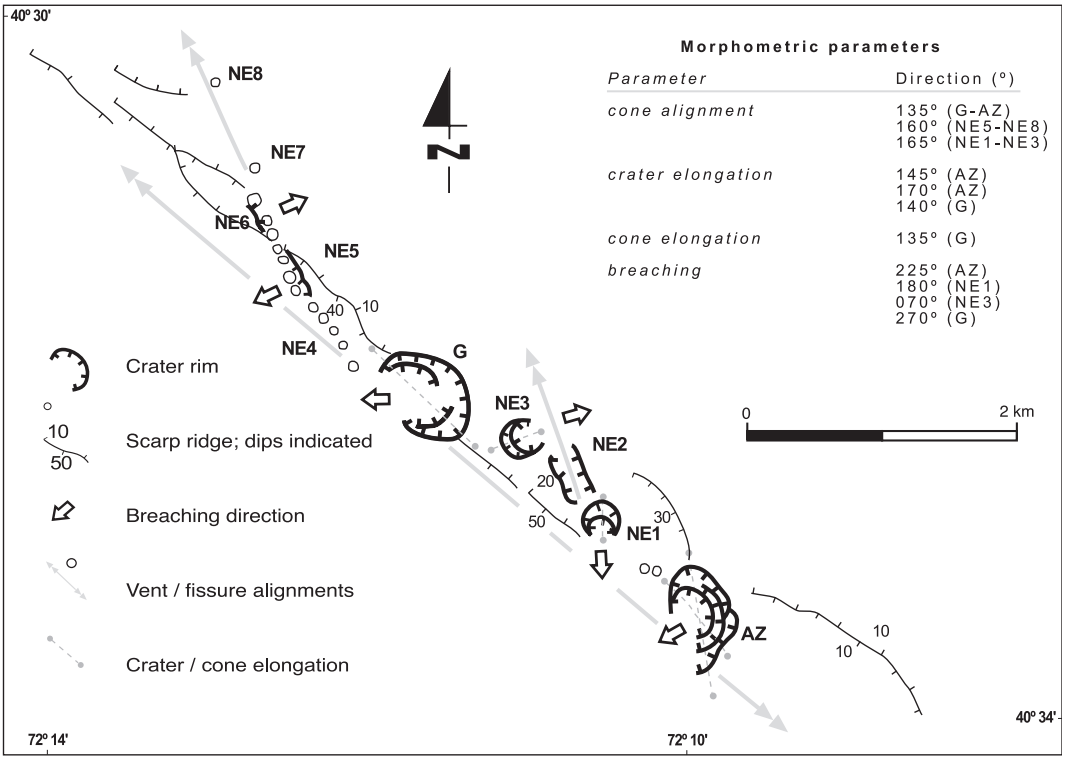

Fig. 4. Geomorphologic map of 1960 fissure in the CCVC and attached values for morphometric parameters. Key as Fig. 2.

aligned in N160–165° direction (Fig. 2). The breaching directions are usually orthogonal to the vent alignments and to the elongation of the corresponding craters. Those located on the main N135° alignment are open toward the south or southwest. The main exception is the Gris crater, the opening of which is toward the west. However, the centres located in N160–165° alignments, on the internal flank of the ridge (NE2; NE4), are open toward the northeast or constitute only fissures without individual craters.

6. Structural analysis

In the absence of data gathered from direct instrumental monitoring, we used the morphologic characteristics of the vents to rebuild the structural conditions during the eruptive cycle. Traditionally, authors such as Nakamura (1977) have considered that the alignment of volcanic centres to be parallel to the maximum horizontal stress (σ_{hmax}). Assuming that the volcanic centres are the surface expression of near vertical feeder dikes, the $\sigma 3$ (minimum stress axis) should be horizontal (and perpendicular to the dikes) with σ_{hmax} corresponding to $\sigma 1$ or $\sigma 2$ (Emmerman and Marrett, 1990). If σ_{hmax} corresponds to $\sigma 2$, the arc tectonics is extensional; if σ_{hmax} corresponds to $\sigma 1$ (with $\sigma 3$ lying on the horizontal plane), the arc tectonics is strike-slip. The focal mechanism deduced by Cifuentes (1989) for 1960 thrust earthquake (Fig. 1) and the related coseismic deformation (Plafker and Savage, 1970) suggests that $\sigma 3$ was E–W, and therefore, σ_{hmax} would have been NS. If σ_{hmax} corresponds to $\sigma 2$ or $\sigma 1$ is hard to constrain. Nevertheless, the small amount of shortening near the N–S direction recorded in the geodetic network after the 1960 earthquake (Plafker and Savage, 1970), the absence of N–S normal faults at the first eruptive stage and the parallel array of secondary fissures suggest a horizontal N–S $\sigma 1$ and then, a strike-slip stress regime. The latter is different to the widespread Quaternary transpressional setting of the entire volcanic arc described by Lavenu and Cembrano (1999) for Southern Andes.

On the other hand, recent works show that volcanic alignment parallel to σ_{hmax} is only the simplest scenario, applicable primarily to isotropic materials showing, for example, good correlations in flank cones on stratovolcanoes (e.g., Delaney et al., 1986; Emmerman and Marrett, 1990; Lister and Kerr, 1991; Glazner et al., 1999). Nevertheless, ancient faults could act as ascent pathways for magmas modifying the geometry of volcanic alignments and their morphological features. The faults related to volcanic vents are commonly blind but analogue models developed by Tibaldi (1995) show good empirical correlation between several morphologic parameters of the cones and craters (alignment, breaching directions, elongation of crater and cone base) and the geometry of the underlying fault plane. This relationship is stronger if the elongation of craters is considered, together with the ellipticity of the cone bases and of the nested craters. The relationship is less evident with respect to the displacement of the faults or the stress regime (Tibaldi, 1995) although there is a good correspondence of normal faults to perpendicular breaching directions of the cones and strike-slip faults to parallel breaching directions. Then, vent morphometry is not enough to interpret the state of stress of a region, but it provides some insight into it in absence of direct measures. Applying Tibaldi's results, we can assume that the 1960 fissure eruption was controlled by a structure composed of two subvertical bent segments in which concavity to the northeast suggests a slight northeast dipping geometry. In addition, some breaching directions oblique to the fissure could be related to an early shear-extensional condition (oblique opening) at the first eruptive stage while they suggest almost pure extensional behaviour (orthogonal opening) at the final effusive phase. The breaching direction of the Gris crater, the first active one and the largest of the entire eruption, may indicate the sense of the oblique displacement at the early stage of the eruptive cycle (Fig. 4). In addition, on the near N160–165° segments (stage 3), small normal fault scarps can be observed. Then, we can assume that, despite the topographic conditions, the geomorphological criteria provide some partial information about the coeval state of stress. In the CCVC, the main 1960 crater alignment (N135°) is parallel to a chain of postglacial domes so that the prior topography was constrained by the position of their feeder dikes and the overall Holocene vents lie on the western scarp of the graben which coincides with the trace of a regional fault (Río Iculpe fault). Thus, from the geodetic data and the strain model of

Barrientos (1994) together with the morphometric analysis, we can assume that the underlying fault was an ancient reactivated structure, at least at the first eruptive stage. For proposing a dynamical model, we appeal to some concepts derived from the theory of fractures and hydraulic fracturing. If the propagation of strain from the coastal zone toward the interior of the continent during the earthquake actually occurred as Barrientos (1994) calculated (Fig. 5), then the CCVC area was affected by an E–W extension with small N–S contraction defining a strike-slip regime, as it was stated before. Then, the instantaneous stress axis would be E–W ($\sigma 3$) and N–S ($\sigma 1=\sigma_{hmax}$).

Following the simple model proposed by Byerlee (1978) and Sibson (1985), improved after by Ivins et al. (1990), Yin and Ranalli (1992), Huyghe and Mugnier (1992) and Morris et al. (1996), an oblique NW structure (N135°) is moderately well oriented for a reactivation with an angle of $\theta r=45°$ from $\sigma 1$. This conclusion is confirmed by a quantitative analysis made throughout a software developed by Tolson et al. (2001) that considers other physical conditions for reactivation. The optimal angle of reactivation (angle between the maximum stress axis and the fault plane) is $\theta r=26.5°$ for a coefficient of static friction $\mu=0.75$ (Fig. 6a; Sibson, 1985). We stated for the 1960 earthquake that in the horizontal

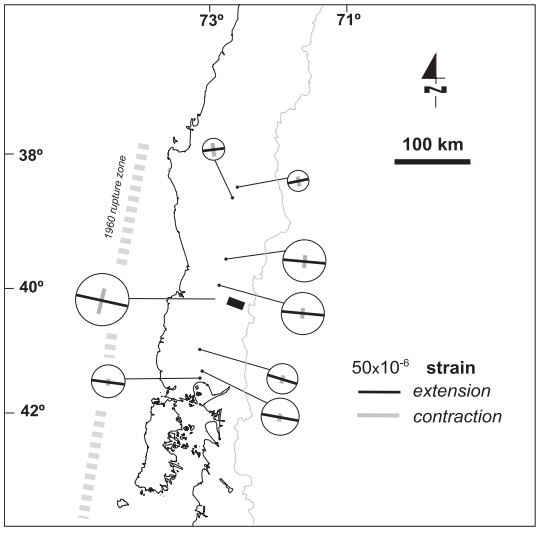

Fig. 5. Deviatoric strains for coseismic deformation calculated by Plafker and Savage (1970) from a geodetic triangulation along the Central Valley of Chile, in front of the rupture zone of 1960 earthquake. Circles are proportional to the amount of extension (adimensional scale bar for 5×10^{-6} strain for reference); orthogonal contraction at the same scale.

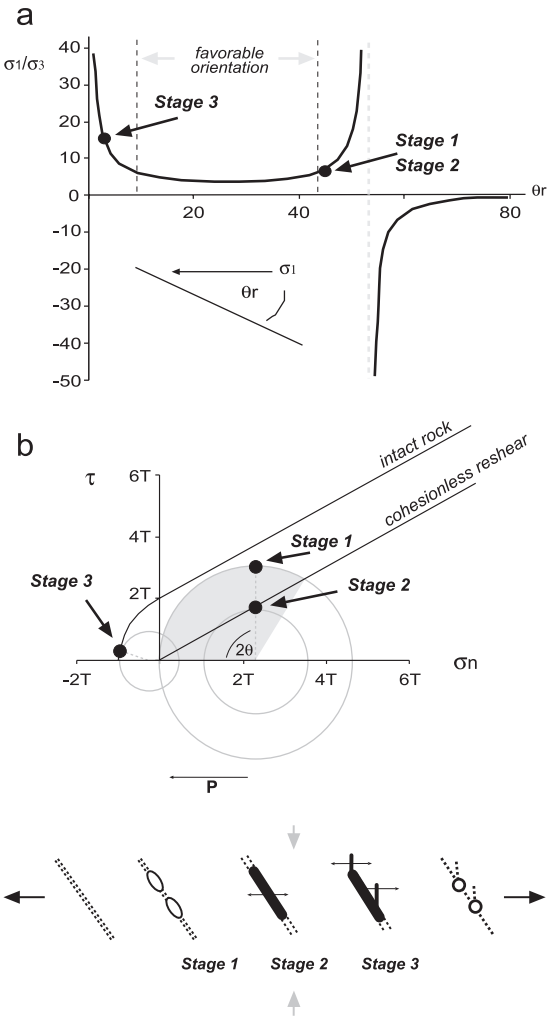

Fig. 6. (a) Effective stress diagram (modified from Sibson, 1985) showing the way of eruptive cycle and the structural conditions from reshear (stage 1 to stage 3). (b) Mohr diagram (shear stress [τ] against effective normal stress [σ_n] normalized to tensile strength [T]) with composite failure envelope for intact rock, reshear condition (Sibson, 1985) for a cohesionless fault and possible macroscopic modes of brittle failure at stage 1, stage 2 (shear-extensional; oblique opening) and stage 3 (extensional-shear, orthogonal opening). Decreasing and increasing effect of fluid (magma) pressure is indicated. Stage 1 correspond to a critical condition but dashed line circle shows a more general scenario for the first stage where all planes between 0 and 2θ (grey shaded) could be reactivated. Sketch below shows the evolution of the fissure (see text for details). Black arrows indicate ongoing tension ($\sigma 3$) and grey arrows correspond to compression ($\sigma 1$) according to geodetic data (Plafker and Savage, 1970).

plane, $\sigma 1=\sigma_{hmax}$ is N–S and $\sigma 3$ is E–W. In the case of 1960 eruption, the condition of reactivation would be reached with a ratio of effective stress of $\sigma 1'/\sigma 3'$ near 7 (with $\sigma 1'=\sigma 1-P$; $\sigma 3'=\sigma 3-P$ with P being the fluid pressure and $\mu=0.75$) (Fig. 6b). This condition can be reached more easily with small values for the coefficient of static friction and the presence of a fluid pressure, a typical feature in an active geothermal field. Other physical conditions, as the depth, were considered by Tolson et al. (2001). Then, assuming a linear relationship between stress and strain, we can obtain a maximum value for $\sigma 3$ of -4 MPa if we consider a 40×10^{-6} strain as Barrientos (1994) calculated and a Young modulus of 1×10^{10} Pa (Turcotte and Schubert, 1982). Barrientos (1994) only considered the main contribution of displacement in E–W direction over the thrust plane for the strain propagation. Nevertheless, the weak N–S compressive stress increases the dextral shear component over the NW fault. Fig. 6b shows a major Mohr's circle that does not reach the Navier–Coulomb envelope for fracture intact rocks. For this non-optimum state of stress, faults with $0<\theta r<60^\circ$ ($0<2\theta r<120^\circ$) could be reactivated depending of their cohesion. At the second eruptive stage, the stress drop and the magma injection along the fault plane would favour the condition for extensional-shear allowing magma drainage to the surface. The arrest of the dyke could increase the fluid pressure favouring new, near pure extensional hydraulic fractures. The dynamic solution would be, initially (stage 1), the reactivation of a NW fault as a dextral shear-extensional failure. However, once the magma occupies the fissure and the explosive phase of the eruptive cycle begins, the pressure drops allowing effusive magma drainage (stage 2) and after a quiescence period, the conditions would vary until they allow the generation of a new, near pure extensional failure, this time near parallel to the σ_{hmax} of NS direction as an hydraulic (magma) fracture (Stage 3; Fig. 6b).

7. Discussion

An instrumental analysis of the instantaneous coeval deformation during an eruptive cycle is the only way to directly constrain the feasibility of the morphologic and structural analysis commented herein. Therefore, our analysis is based on inferences and the argumentative line is robust but speculative. On the other hand, the studied event represents a unique case in the geodynamic context of the SSAVZ (37–46°S) of the Andes and the kinematics considerations cannot extend to the 'normal' state of the volcanic arc. In fact, the microtectonic analysis (*striae*) of mesoscopic structures and focal mechanism of crustal earthquakes suggests opposite conditions of strain (dextral N–S transpression in the volcanic arc as a whole, with dextral strike-slip in the Liquiñe–Ofqui Fault and sinistral strike-slip in NW structures (e.g., Assumpçao, 1992; Lavenu and Cembrano, 1999), that would have been reversed during the 1960 earthquake.

7.1. 1921–1922 eruption

A point of additional conflict is indicated by the December 1921–February 1922 fissure eruption. That eruption also produced rhyodacitic lava flows (68–71% SiO_2) with vents aligned on a NW fissure joined with the ring faults inside the Cordillera Nevada caldera. Nevertheless, in December 1921, there was no record of any noticeable earthquake in the region and that eruption should be assumed as an event that took place during the 'normal' stress regime of the volcanic arc. However, the expected extensional fractures in the dextral–transpressional regime must be in NE direction. Then, local deviations of a complex stress field or a fluid pressure-controlled behaviour of the magma ascent giving a non-Andersonian setting can be assumed as well. So, as in other natural phenomena, similar effects can be obtained from different causes.

7.2. '*Valve*' *faults and seismic pumping*

The application of the reshear criterion of Byerlee (1978) and Sibson (1985) raises additional questions. For example, the coseismic deformation during the 1960 earthquake found other volcanic alignments that had an equivalent orientation ($\theta r=45^\circ$) to the reshear criterion. In fact, NE–SW-oriented structures that align the monogenic cones at Carrán–Los Venados (40°S) or Antillanca (41°S) groups are located only about 10 km north and south of the CCVC,

respectively. In an even more favourable orientation for reactivation would be the Liquiñe–Ofqui Fault, which parallels the Chile–Peru trench and the expected maximum horizontal stress. Nevertheless, both types of structures did not demonstrate reactivation during the 1960 event. We suppose then that these faults were sealed and would act like 'valves' (Sibson et al., 1988) by dynamic loading during other types of seismic events such as those that characterise the current stress field as a dextral transpressional regime (e.g., Chinn and Isacks, 1983; Barrientos and Acevedo, 1992). So, we propose that the NW–SE fault systems, where the CCVC is located, are regionally favourable to steady-state magma transport, storage and their subsequent differentiation, an idea enunciated before in other terms by Cembrano and Moreno (1994). Thus, the magma is maintained in the upper crust levels, where the faults could act as 'pumps' (Sibson et al., 1988) during seismic events. In that way, the upper level processes (fractional crystallization; hydrothermalism) would increase the fluid pressure near the structure facilitating its reactivation and the renewal of the magma ascent.

7.3. Remote seismic triggering of seismicity and volcanism

The relationship between distant earthquakes, remote remote seismicity and volcanic eruptions has been analysed from different perspectives. From a statistical approach, Blot (1965), Acharya (1982) and Linde and Sacks (1998) studied data collections of major subduction (thrust) earthquakes and volcanic eruptions with contradictory results. Despite the biased sample method, Blot (1965) and Acharya (1982) conclude an unidirectional relation from big eruptions to earthquakes. On the other hand, Linde and Sacks (1998) proposed a causal relationship between Mw>7 earthquakes and eruptions in a radius of 250 km from the seismic source based on a bubble rising model for propagation of dynamic stress. Nevertheless, these authors neglect the pair earthquake-eruption discussed herein, maybe the clearest example of a causal relation between this type of events. A more complete revision of earthquake interactions was published in a special issue of the Journal of Geophysical Research (Stress triggers, stress shadows, and implications for seismic hazard, 1998, V.101, No.B10). There, several papers (e.g., Harris, 1998; Toda et al., 1998; Harris and Simpson, 1998; Nostro et al., 1998) demonstrate Coulomb stress change and other methods for a calculation of dynamic and static stress over active fault as consequence of an earthquake. Although we do not have any seismic parameter of the shear-extensional or extensional faults in the CCVC eruption, the strong spatial and time relationship between the thrust earthquake and the fissure eruption can be analysed as a consequence of dynamic stress propagation. Dynamic strain could be translated to static strain, at local scale, by rectified diffusion (Brodsky et al., 1998) increasing magma pressure that allows reshearing of an ancient fault. In this conceptual framework, the brittle failure theory helps to understand the geometry and evolution of this special but unknown fissure eruptive event.

8. Conclusions

Almost 2 days after the largest instrumentally recorded earthquake registered in the world, in May 1960, a noticeable fissure eruption of rhyodacitic magma took place in the CCVC, ca. 240 km to the east of the rupture zone. The dynamic stress and the general extension propagated toward the continent as a result of the thrust in the subduction zone would have favoured the structural conditions for the evacuation of magma stored in a shallow reservoir. The presence of remarkable NW structures, oblique to the margin, which is typical of the SAVZ and particularly of the CCVC, necessarily forces one to look for a mechanism to explain their reactivation as a response of the whole structural system. In addition, in 1960, new structures were not generated in other places of the volcanic arc, according to the direction of the E–W extension inferred from the geodetic record. Besides, in the CCVC, the fluid pressure increased by the presence of silicic magma near the surface would have facilitated the reactivation of the NW structure, moderately well oriented for the displacement. Hence, the eruptive cycle would have begun by 'seismic pumping' of magma after a dextral shear-extensional displacement of the NW structure as a consequence of a strike-slip regime. After the blockage of first displacement (E–W opening), the

deformation continued with the opening of NNW near pure extensional failure, this time nearly parallel to the expected maximum horizontal stress as hydraulic fractures. Although the lack of instrumental record precludes possibilities to verify the inferences presented herein, the morphometric, structural and volcanological analysis allows reconstruction of the most likely prevailing structural condition during the 1960 fissure eruption. The causal relationship described, although exceptional in the geodynamic evolution of the western South American margin, indicates the relevance of peculiar episodes in the construction of the geologic record.

Acknowledgements

This work is part of a research of the first author on the relationship between volcanism and tectonics in the Southern Andes, a collaborative project of SERNAGEOMIN (Chile) and IRD-Université Paul Sabatier (France). Fieldwork has been supported by Fondecyt 1960885 (HM, LL) grant. Stratigraphic data of the 1960 tephra-fall have been also obtained through Fondecyt 1960186 (JN, HM, LL) grant. The authors are grateful to R. Scandone, P. Segall, and D. Hill for their critical revision of an early version. M. Neri, E. Parfitt and specially S. Alaniz-Alvarez are kindly acknowledged as reviewers. This work is a contribution to the Volcanic Hazards Project of SERNAGEOMIN (Chile).

References

Acharya, H., 1982. Volcanic activity and large earthquakes. J. Volcanol. Geotherm. Res. 86, 335–344.

Alaniz-Alvarez, S., Nieto-Samaniego, A., Ferrari, L., 1998. Effect of strain rate in the distribution of monogenetic and polygenetic volcanism in the Transmexican volcanic belt. Geology 26, 591–594.

Anderson, E.M., 1951. The Dynamics of Faulting, 2nd ed. Oliver and Boyd, pp. 1–191.

Assumpçao, M., 1992. The regional intraplate stress field in South America. J. Geophys. Res. 97, 11,889–11,903.

Bahar, I., Girod, M., 1983. Controle structural du volcanisme indonesien (Sumatra, Java–Bali); application et critique de la methode de Nakamura. Bull. Soc. Geol. Fr. 7, 609–614.

Barrientos, S., 1994. Large thrust earthquakes and volcanic eruptions. Pure Appl. Geophys. 142, 225–237.

Barrientos, S., Acevedo, P., 1992. Seismological aspects of the 1988–1989 Lonqimay (Chile) volcanic eruption. J. Volcanol. Geotherm. Res. 53, 73–87.

Barrientos, S., Ward, S.N., 1990. The 1960 Chile earthquake: coseismic slip from surface deformation. Geophys. J. Int. 103, 589–598.

Bellier, O., Sébrier, M., 1994. Relationship between tectonism and volcanism along the Great Sumatran Fault deduced by SPOT image analyses. Tectonophysics 233, 215–231.

Berninghausen, W.H., 1962. Tsunamis reported from the west coast of South America. Seismol. Soc. Am., Bull. 52, 915–921.

Blot, C., 1965. Relation entre les séismes profonds et les éruptions volcaniques au Japon. Bull. Volcanol. 28, 25–64.

Brodsky, E.E., Sturtevant, B., Kanamori, H., 1998. Earthquakes, volcanoes, and rectified diffusion. J. Geophys. Res. 103, 23827–23838.

Byerlee, J.D., 1978. Friction of rocks. Pure Appl. Geophys. 116, 615–626;
Byerlee, J.D., 1978. Friction of rocks. J. Geophys. Res. 103, 23,827–23,838.

Campos, A., Moreno, H., Muñoz, J., Antinao, J., Clayton, J., y Martin, M., 1998. Area de Futrono-Lago Ranco, Región de los Lagos. Servicio Nacional de Geología y Minería, Mapas Geológicos No. 8, 1 mapa escala 1:100.000. Santiago.

Casertano, L., 1962. Sui fenomini sismo-vulcanici del Sud del Chile. Annali Osservatorio Vesuviano 4 (serie 6) Nápoles.

Cembrano, J., Moreno, H., 1994. Geometría y naturaleza contrastante del volcanismo cuaternario entre los 38°S y 46°S: Dominios compresionales y tensionales en un régimen transcurrente? Congr. Geol. Chil. Actas 1 (7), 240–244.

Cembrano, J., Hervé, F., Lavenu, A., 1996. The Liquiñe–Ofqui fault zone: a long-lived intra-arc fault system in southern Chile. Tectonophysics 259, 55–66.

Chinn, D., Isacks, B., 1983. Accurate source depths and focal mechanisms of shallow earthquakes in Western South America and the New Hebrides Island arc. Tectonics 2, 529–563.

Cifuentes, I.L., 1989. The 1960 Chilean earthquakes. J. Geophys. Res. 94, 665–680.

Delaney, P.T., Pollard, D.D., Ziony, J.I., Mckee, E.H., 1986. Field relations between dykes and joints: emplacement processes and paleostress analysis. J. Geophys. Res. 91, 4920–4938.

DeMets, C., Gordon, R., Argus, D., Stein, S., 1994. Effect of recent revisions to the geomagnetic reversal time scale on estimates of current plate motions. Geophys. Res. Lett. 21, 2191–2194.

Dhont, D., Chorowicz, J., Yürür, T., Froger, J.L., Köse, O., Gündogdu, N., 1998. Emplacement of volcanic vents and geodynamics of Central Anatolia, Turkey. J. Volcanol. Geotherm. Res. 62, 207–224.

Duda, S.J., 1963. Strain release in the circum-Pacific belt, Chile, 1960. J. Geophys. Res. 68, 5,531–5,544.

Eaton, J.P., Richter, D.H., Ault, W.U., 1961. The tsunami of May 23, 1960, on the island of Hawaii. Seismol. Soc. Am., Bull. 51, 135–157.

Emmerman, S., Marrett, R., 1990. Why dikes? Geology 18, 231–233.

Gerlach, D., Frey, F., Moreno, H., López, L., 1988. Recent

volcanism in the Puyehue–Cordón Caulle Region, Southern Andes, Chile (40.5°S): petrogenesis of evolved lavas. J. Petrol. 29, 333–382.
Glazner, A., Bartley, J., Carl, B., 1999. Oblique opening and noncoaxial emplacement of the Jurassic Independence dike swarms. J. Struct. Geol. 21, 1275–1283.
Gutenberg, B., 1956. The energy of the earthquakes. Q. J. Geol. Soc. London. 112, 1–14.
Harris, R., 1998. Introduction to special section: stress triggers, stress shadows, and implications for seismic hazard. J. Geophys. Res. 103, 24,347–24,358.
Harris, R., Simpson, R., 1998. Suppression of large earthquakes by stress shadows: a comparison of Coulomb and rate-and-state failure. J. Geophys. Res. 103, 24,439–24,451.
Hubbert, M.K., Rubey, W.W., 1959. Role of fluid pressure in the mechanics of overthrust faulting. Geol. Soc. Am. Bull. 70, 115–205.
Huyghe, P., Mugnier, J.L., 1992. The influence of the depth on reactivation in normal faulting. J. Struct. Geol. 14, 991–998.
Ivins, E.R., Dixon, T.H., Golombek, M.P., 1990. Extensional reactivation of an abandoned thrust: a bound on shallowing in the brittle regime. J. Struct. Geol. 12, 303–314.
Kanamori, H., 1977. The energy release in great earthquakes. J. Geophys. Res. 82, 2981–2987.
Kanamori, H., Cipar, J.J., 1974. Focal process of the great Chilean earthquake, May 22, 1960. Phys. Earth Planet. Inter. 9, 128–136.
Katsui, J., Katz, H., 1967. Lateral fissure eruptions in the Southern Andes of Chile. Faculty of Science Series, vol. 4, pp. 433–448. Japan.
Lara, L., Rodriguez, C., Moreno, H., Pérez de Arce, C., 2001. Geocronología K–Ar y geoquímica del volcanismo plioceno superior-pleistoceno de los Andes del Sur (39°–42°S). Rev. Geol. Chile 28, 67–90.
Lara, L.E., Matthews, S., Pérez de Arce, C., Moreno, H., 2003. Evolución morfoestructural del Complejo Volcánico Cordón Caulle (40°S): evidencias geocronlógicas $^{40}Ar/^{39}Ar$. Congreso Geológico Chileno, vol. 10. Actas, Concepción.
Lavenu, A., Cembrano, J., 1999. Compressional and traspressional-stress pattern for Pliocene and Quaternary brittle deformation in fore arc and intra-arc zones (Andes of Central and Southern Chile). J. Struct. Geol. 21, 1669–1691.
Linde, A.T., Sacks, I.S., 1998. Triggering of volcanic eruptions. Nature 395, 888–890.
Lister, J.R., Kerr, R.C., 1991. Fluid-mechanical models of crack propagation and their application to magma transport in dikes. J. Geophys. Res. 96, 10,049–10,077.
Moreno, H., 1977. Geología del área volcánica Puyehue-Carrán en los Andes del sur de Chile. Memoria para optar al título de geólogo. Departamento de Geología, Universidad de Chile.
Morris, A., Ferril, D.A., Hendeson, D.B., 1996. Slip-tendency análisis and fault reactivation. Geology 24, 275–278.
Nakamura, K., 1977. Volcanoes as possible indicators of tectonic stress orientation: principle and proposal. J. Volcanol. Geotherm. Res. 2, 1–16.
Nostro, C., Ross, S., Cocco, M., Belardinelli, M.E., Marzochi, W., 1998. Two-way coupling between Vesuvius eruptions and southern Apennine earthquakes, Italy, by elastic stress transfer. J. Geophys. Res. 103, 24,439–24,451.
Peña, P., Fuentealba, G., 2000. Antecedentes preliminares de sismicidad asociada al complejo volcánico activo Cordón Caulle, Andes del Sur (40,5°S). Congreso Geológico Chileno, vol. 9, pp. 52–53. Actas 2.
Plafker, G., Savage, J.C., 1970. Mechanism of Chilean earthquakes of May 21 and May 22, 1960. Geol. Soc. Am. Bull. 81, 1001–1030.
Saint Amand, P., 1961. Los Terremotos de Mayo-Chile 1960, an eyewitness account of the greatest natural catastrophe in recent history. U.S. Naval Ordinance Test Station, Technical article 14, 39 p. China Lake.
Sibson, R., 1985. A note on fault reactivation. J. Struct. Geol. 7, 751–754.
Sibson, R., 1987. Earthquake rupturing as a mineralizing agent in hydrothermal systems. Geology 15, 701–704.
Sibson, R., 1996. Structural permeability of fluid-driven fault-fracture meshes. J. Struct. Geol. 18, 1031–1042.
Sibson, R., 2000. A brittle failure mode plot defining conditions for high-flux flow. Econ. Geol. 95, 41–48.
Sibson, R., Robert, F., Poulsen, K.H., 1988. High-angle reverse faults, fluid-pressure cycling, and mesothermal gold–quartz deposits. Geology 16, 551–555.
Sievers, H., Villegas, G., Barros, G., 1963. The seismic sea wave of 22 May 1960 along Chilean Coast. Seismol. Soc. Am., Bull., 1125–1190.
Smylie, D.E., Mansinha, L., 1968. Earthquakes and the observed motion of rotation pole. J. Geophys. Res. 73, 7,661–7,663.
Takada, A., 1994. The influence of regional stress and magmatic input on styles of monogenetic and polygenetic volcanism. J. Geophys. Res. 99, 13,563–13,573.
Tibaldi, A., 1995. Morphology of pyroclastic cones and tectonics. J. Geophys. Res. 100, 24,521–24,535.
Toda, S., Stein, R., Reasenberg, P., Dietrich, J., Yoshida, A., 1998. Stress transferred by 1995 Mw=6.9 Kobe, Japan shock: effect on the aftershocks and future earthquake probabilities. J. Geophys. Res. 103, 24,543–24,565.
Tolson, G., Alaniz-Alvarez, S.A., Nieto-Samaniego, A., 2001. ReActiva, a plotting program to calculate the potential of reactivation of preexisting planes of weakness. Instituto de Geología, Universidad Autónoma de México. http://geologia.igeolcu.unam.mx/Tolson/Software/ReActivaV24En.exe.
Turcotte, D., Schubert, G., 1982. Geodynamics, Application of Continuum Physics to Geological Problems. John Wiley and Sons, New York.
Veyl, C., 1960. Los fenómenos volcánicos y sísmicos de fines de Mayo de 1960 en el sur de Chile. Universidad de Concepción, Instituto Central de Química, Concepción, 42 pp.
Ward, S.N., 1984. A note on lithospheric bending calculations. Geophys. J. R. Astron. Soc. 78, 241–253.
Weischet, W., 1963. Further observations of geologic and geomorphic changes resulting from the catastrophic earthquake of May 1960, in Chile. Seismol. Soc. Am., Bull. 53, 1237–1257.
Yin, Z.M., Ranalli, G., 1992. Critical stress difference, fault orientation and slip direction in anisotropic rocks under non-Andersonian stress systems. J. Struct. Geol. 14, 237–244.